Am J Transl Res 2021;13(2):565-584
www.ajtr.org /ISSN:1943-8141/AJTR0120479

Original Article

Tanshinone IIA regulates fibroblast proliferation and migration and post-surgery arthrofibrosis through the autophagy-mediated PI3K and AMPK-mTOR signaling pathway

Zhen Zhang[1*], Dongming Zhu[1], Xiaobo Zhang[1], Yun Liu[3], Jingcheng Wang[3], Lianqi Yan[2,3*]

[1]Dalian Medicial University, Dalian 116044, Liaoning, China; [2]Central South University, Changsha 410012, Hunan, China; [3]Department of Orthopedics, Northern Jiangsu People's Hospital, Clinical Medical College of Yangzhou University, Yangzhou 225001, Jiangsu, China. [*]Equal contributors.

Received August 17, 2020; Accepted November 29, 2020; Epub February 15, 2021; Published February 28, 2021

Abstract: Post-surgery arthrofibrosis is one of the most restrictive factors in the development of intra-articular surgery and has presented tremendous obstacles for most orthopaedic surgeons. Tanshinone IIA (Tan IIA), a key active ingredient of Den-shen, has been used to treat fibrosis-related diseases, such as pulmonary, hepatic and myocardial fibrosis. In the present study, we aimed to investigate the effects of Tan IIA on post-surgery arthrofibrosis *in vivo* and *in vitro*. Histological analysis indicated that topical application of Tan IIA (10 mg/mL) could significantly alleviate postsurgery arthrofibrosis in rabbits. Immunohistochemistry results showed that proliferating cell nuclear antigen (PCNA) and tubulin protein expression was inhibited, whereas LC3 was activated *in vivo*. *In vitro*, EdU and flow cytometry assays demonstrated that Tan IIA could inhibit fibroblast proliferation by arresting cells in G2 phase. Scratch, Transwell and cytoskeleton protein immunofluorescence assays revealed that fibroblast migration was attenuated. Interestingly, LC3 immunofluorescence staining and transmission electron microscopy indicated that autophagy flux could be induced in fibroblasts by Tan IIA. However, the inhibitory effects of Tan IIA against fibroblast proliferation and migration were partially restored when fibroblast autophagy was suppressed after combined treatment with the autophagy inhibitor 3-methyladenine (3-MA). Finally, the expression of p-mTOR was suppressed in a dose-dependent manner after Tan IIA treatment but partially restored when Tan IIA treatment was combined with 3-MA intervention. The inhibitory effect of Tan IIA against fibroblast proliferation and migration may be related to autophagy induction mediated by the PI3K and AMPK-mTOR signaling pathway.

Keywords: Tanshinone IIA, postsurgery arthrofibrosis, autophagy, proliferation, migration, mTOR signaling

Introduction

Post-surgery arthrofibrosis has become a challenge for most orthopaedic surgeons. Clinical reports indicate that approximately 4% of patients require interventions as a result of arthrofibrosis induced by articular surgery [1-4]. After joint surgery, local inflammation occurs in the surgical area and releases inflammatory factors. Fibroblasts can aggregate, proliferate and secrete a large amount of ECM [5]. Many clinical trials and fundamental studies aimed at preventing this problem have been conducted. Although some pharmaceutical agents have been confirmed to ameliorate intra-articular adhesion in animals, it is still difficult to apply these agents clinically due to their obvious side effects and the difficulty in their translation into clinical application [5]. Therefore, new pharmaceutical agents that can be topical administered with fewer side effects, need to be discovered.

In recent decades, research on "self-eating", a process by which cells preserve homeostasis through the degradation of their own components, has aroused strong interest. Additionally, the notion that autophagy is involved in many diseases has been confirmed [6, 7]. Studies have shown that autophagy is associ-

ated with fibrosis [8, 9]. One study showed that artesunate ameliorated orthopaedic post-operation fibrosis in animals by regulating autophagy [9].

The PI3K-mTOR pathway, a classical autophagy pathway, regulates cell proliferation, survival, and migration [10, 11]. AMP-activated protein kinase (AMPK), which plays a role in regulating energy to mediate cell proliferation, migration and homeostasis, is connected to autophagy processes through the modulation of mTOR [12, 13].

Growing evidence has demonstrated that many compounds extracted from organisms in nature may act as new anti-fibrosis drugs based on their ability to modulate autophagy [14]. Tanshinone IIA (Tan IIA) is a naturally occurring phenanthraquinone compound extracted from *Salvia miltiorrhiza Bunge* that is widely used in traditional Chinese medicine. Tan IIA possesses many pharmacological activities, including its anti-inflammatory, immune-regulation and anti-fibrosis activities [15, 16]. Furthermore, Tan IIA was found to promote autophagy in myeloid cells and H_9C_2 cells to regulate proliferation and apoptosis via the PI3K/AKT/mTOR and AMPK/mTOR pathways [17, 18].

These previous studies indicate that Tan IIA can promote autophagy and exert anti-fibrotic effects, which may be useful for treating surgery-induced intra-articular fibrosis. However, the effect of Tan IIA on arthrofibrosis has not yet been reported. In this study, we aimed to examine the ability of Tan IIA to ameliorate rabbit arthrofibrosis *in vivo* and regulate fibroblast proliferation, migration and autophagy. We also further explored the relationship between these processes *in vitro*.

Materials and methods

Animals and reagents

Thirty-six male New Zealand rabbits weighing 2.5 to 3.0 kg were obtained from the Yangzhou University Experimental Animal Center (Yangzhou, China). Tan IIA (purity, 98%) was purchased from Aladdin (Shanghai, China). The rabbit experiment protocols were approved by the Animal Ethics Committee of Yangzhou University. Rabbits were randomly divided into three groups: the control group and 5.0 mg/mL and 10 mg/mL Tan IIA groups [19].

Arthrofibrosis model establishment

A rabbit knee arthrofibrosis model was established according to a previous study [20]. Briefly, anaesthesia was induced. The skin was prepared and the surgical area was disinfected. Then, an approximately 10-mm diameter area of cortical bone on both sides of the left femoral condyle was removed to expose the cancellous bone, leaving the articular cartilage intact. After satisfactory haemostasis, the wound was covered with cotton pads pre-soaked with Tan IIA at various concentrations for 10 min. Then, the cotton pads were removed, and the articular capsule and skin were closed with silk sutures. Finally, the surgical limbs were fixed in a fully flexed position using Kirschner wires for 28 days. Penicillin (50 mg/kg) was administered intramuscularly for 3 days after the operation.

Haematoxylin and eosin (HE), masson and sirius red (SR) staining

Rabbits were euthanized at the fourth week following the knee operation, after which the entire knee joint was removed and fixed with 10% formalin for 36 h. Then, the decalcified joints were embedded in paraffin. Successive 4-μm transverse sections at the operation area were prepared, and sections were successively stained with HE, Masson's trichrome and SR.

Paraffin section immunofluorescence (IF-P) staining

Immunofluorescence (IF) staining of vimentin (bs-23064R, Bioss, Beijing, China) and fibroblast-specific protein-1 (bs-3759R, Bioss), a protein specific to fibroblasts, was used to detect the fibroblasts in intra-articular fibrosis scar tissue. In brief, the tissue was first deparaffinized and rehydrated, followed by antigen retrieval. Next, the tissue was incubated with primary antibodies for 16 hours (h) at 4°C followed by secondary antibodies (ab150075/ab150073, Abcam, Cambridgeshire, England) for 60 minutes (min) at 25°C. DAPI (C0065, Solarbio, Beijing, China) staining was applied for 10 min, after which the fluorescence signals

were viewed with a fluorescence microscope (Axio-Vert, Zeiss, Germany).

Immunohistochemistry (IHC) analysis

PCNA (bs-2007R, Bioss), tubulin (ba-20694R, Bioss) and LC3B (NB100-2220, Novus, Minnesota, USA) protein expression in intra-articular fibrosis scar tissue was detected with IHC staining. Briefly, deparaffinization, rehydration, and antigen retrieval were performed as previously described, and endogenous peroxidases were removed with 3% H_2O_2. The tissue was incubated with primary antibodies for 12 h at 4°C, followed by incubation with secondary antibody (anti-rabbit IgG) for 60 min at 25°C. Finally, a DAB kit and haematoxylin were used to reveal antibody binding after incubation for the appropriate duration, and signals were viewed with a light microscope (ERC5S, Zeiss).

Cell and cell culture

The human HDF-α cell line was purchased from ScienCell Research Laboratories (California, USA) and cultured in DMEM (Gibco, CA, USA) with 10% FBS (Clarkbio, VA, USA) at 37°C in a 5% CO_2 incubator.

Cell viability assay

Briefly, 1×10^4 cells/well were cultured in a 96-well plate for approximately one day, and triplicate wells were prepared for each group. The cells were treated with Tan IIA at different concentrations (0, 2.5, 5.0, 10, 20, 40, 80 μM) and normal complete medium for an additional 12, 24, 36, or 48 h. Next, 10 μL of CCK-8 (Dojindo, Tokyo, Japan) buffer was added to each well and incubated with the cells at 37°C under 5% CO_2 for an additional 4 h. Finally, the absorbance of the cells at 450 nm was measured with an absorbance microplate reader (Infinite M1000 PRO, Tecan, Switzerland). Cell viability was calculated according to the kit instructions.

EdU assay

Briefly, 1×10^5 cells/well were plated in 24-well plates with diameter a 14-mm diameter coverslip (WHB, Shanghai, China). Tan IIA at various concentrations or 2 mM 3-MA (MCE, New Jersey, United States) was added to the wells for 48 h. Then, 40 μM 5-ethynyl-2'-deoxyuridine (Invitrogen, California, United States) was added to the wells for an additional 2 h. To fix and improve cell membrane permeability, 4% paraformaldehyde and 0.5% Triton X-100 in PBS were applied for 15 min. Hoechst 33342 was used to label cell nuclei. A fluorescence microscope (Axio-Vert, Zeiss) was used to view the signal.

Cell cycle analysis

Cell cycle assays were used to analyse the cell cycle distribution with a Cell Cycle Kit (Beyotime, Shanghai, China). After treatment with Tan IIA at different concentrations for 48 h, the cells were harvested and centrifuged at 1000 r/min for 4 min and then fixed in 70% ice-cold ethanol overnight at 4°C. The cells were resuspended and co-incubated in a propidium iodide (PI) solution (0.4 mL) for half an hour in a 25°C water-bath in the dark. Finally, the cell suspension was used to analyse cell cycle via flow cytometry (MoFlo^{TM} XDP, Beckman, Germany).

Wound closure assay

Fibroblasts were inoculated into a 6-well plate and cultured until the cells covered the entire well surface. Then, 200-uL tips were used to create a scratch in the cell monolayer, and exfoliated cells were washed away with PBS. Next, the complete medium was exchanged for serum-free medium, and cells images were acquired at the 0-h time point. The cells were then photographed at established times with an inverted optical microscope (Axio-Vert A1, Zeiss).

Transwell cell migration assay

Transwell assays can not only reveal cell migratory behaviours but also are used to observe variations in cellular morphology [21]. Briefly, 1×10^5 fibroblasts/mL were suspended in serum-free medium, and 100 μl of the cell suspension was seeded on the top filter membrane and incubated for 10 min. An additional 600 μl of complete medium containing Tan IIA or 3-MA was carefully added to the lower chamber, followed by incubation for 48 h. The cells were fixed with 70% ethanol for 10 min. Then, a cotton-tipped applicator was used to remove the remaining cells and ethanol from the top filter membrane. Next, 0.2% crystal

violet was added to the low chamber and incubated for 15 min at 25°C. After staining, the remaining crystal violet was carefully removed from the top membrane using a cotton-tipped swab, and the cells were gently washed with water. An inverted microscope (Axio-Vert, Zeiss) was used to view the signal.

Cell immunofluorescence (IF-C) imaging analysis

Fibroblasts were inoculated in a 24-well plate with a 14-mm diameter coverslip (WHB) until they grew to 60% to 70% confluence. Then, the cells were treated with Tan IIA at various concentrations for 48 h. Then, the cells were fixed with 4% paraformaldehyde for half an hour, permeabilized with 0.5% Triton X-100 for 10 min, and blocked with 2.5% BSA (Aladdin, Shanghai, China) for half an hour. Primary antibody (Abcam, Cambridge, England) diluted to the recommended proportion was incubated with the cells for 18 h at 4°C, followed by incubation with the corresponding secondary antibody (Abcam, Cambridge, England) for 90 min. Nuclei were stained with DAPI for 10 min. Finally, the samples were photographed with a True confocal system (TCS SP8, Leica, Germany).

Transmission electron microscopy (TEM) analysis

Autophagosome formation is the most direct and important evidence of autophagy, and TEM analysis is regarded as the gold standard for the detection of autophagosomes [22]. In brief, cells were harvested after treatment with Tan IIA or PBS. Then, a pre-chilled 2.5% glutaraldehyde solution was used to fix the cells for 2 h, followed by treatment with a 1% OsO_4 solution for an additional 60 min. Finally, the samples were dehydrated in a gradient ethanol series (70% ethanol for 20 min, 95% ethanol for 20 min, 100% ethanol for 20 min, 100% ethanol for another 20 min), embedded with epon and stained with uranyl acetate and lead citrate. Images were obtained by TEM (Philips TECNAL, Philips, Amsterdam, Netherlands).

Western blot analysis

Briefly, 5×10^5 cells were inoculated into dishes. When cells covered 60% of the area of plates, they were treated with Tan IIA or 3-MA for 48 h. The cells were lysed, and the lysis suspension protein concentration was determined using a Bio-Rad protein assay kit (ChemiDoc MP, Bio-Rad Laboratories, California, USA). Then, 40 ug/well cellular proteins were separated in 8% to 12% SDS-PAGE gels and then transferred onto PVDF membranes. After blocking with 5% milk for 2.5 h, the PVDF membranes were incubated with primary antibodies for 16 h at 4°C, followed by incubation with secondary antibodies for 2 h. An imaging system (ChemiDoc MP, Bio-Rad Laboratories, California, USA) was used to visualize antibody reactivity.

Statistical analysis

Data were analysed using SPSS 17.0 software, and the results are presented as the means ± standard deviations (SDs). Statistical analysis was performed via one-way analysis of variance (ANOVA), followed by Dunnett's test and Tukey's test. In the present study, a *p*-value < 0.05 was used to indicate statistical significance.

Results

Tan IIA ameliorated postsurgery knee arthrofibrosis in rabbits

Vimentin and FSP-1 IF-P staining was used to determine the distribution of fibroblasts in knee arthrofibrosis. The resulting images showed that fibroblasts, the major cell type that filled the arthrofibrosis scars, presented a uniform distribution in the field of vision (**Figure 1A**). In contrast, after treatment with Tan IIA, the number of cells and dense fibrotic tissue in the scar was decreased based on HE staining (**Figure 1B**). Masson and SR staining was used to measure the degree of collagen synthesis in knee arthrofibrosis after the topical administration of Tan IIA in rabbits. The Masson and SR staining results indicated that the collagen synthesis in knee arthrofibrosis was ameliorated in a dose-dependent manner with the application of Tan IIA (**Figure 1B**, **1C**). The SR staining results showed that collagen I fibres (yellow or red) and collagen III fibres (green) were reduced in the Tan IIA-treated group. In addition, SR staining suggested that collagen I and III are the major collagen components (**Figure 1B**).

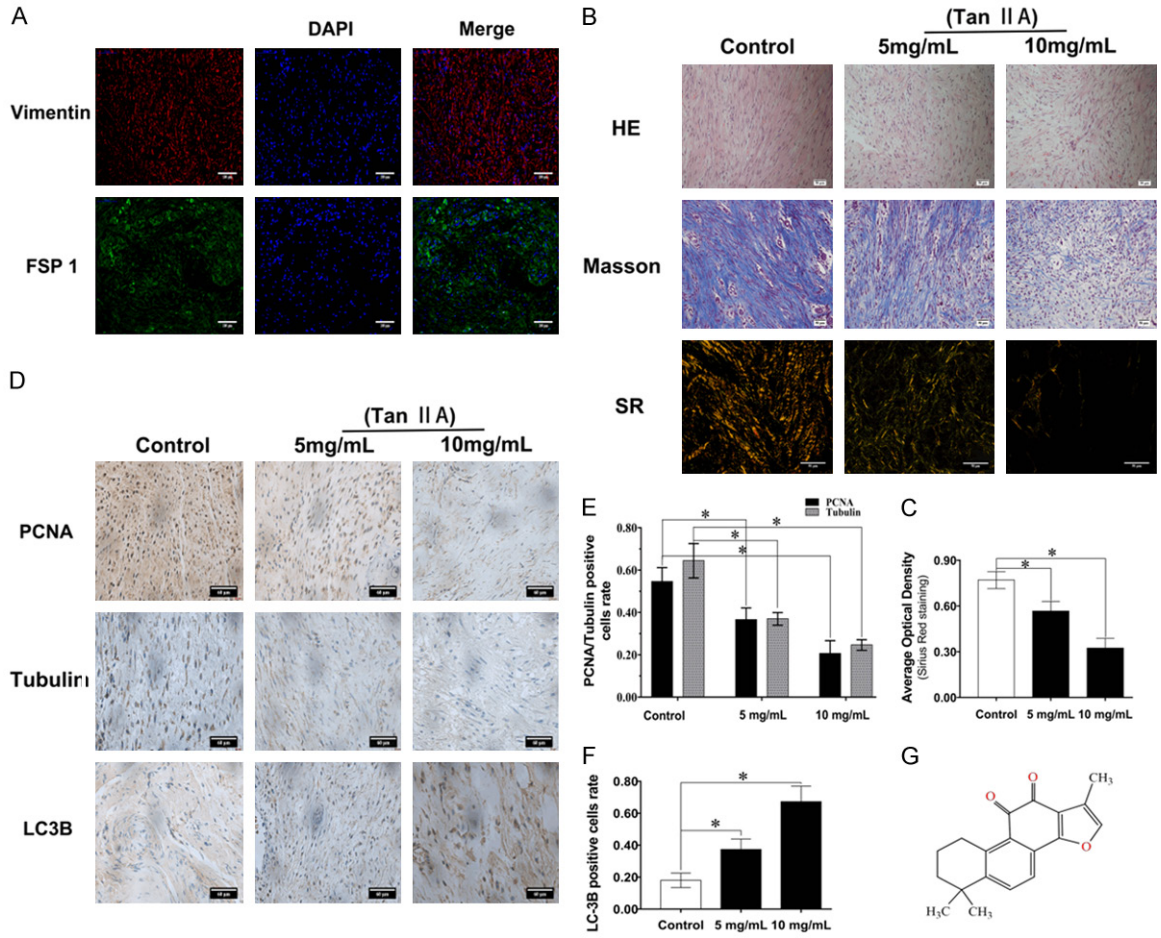

Figure 1. Tan IIA alleviated post-surgery arthrofibrosis *in vivo*. (A) Immunofluorescence staining of vimentin and FSP-1 *in vivo* showed a linear signal, with vimentin (red) and FSP-1 (green) localized in a fibrous structure. DAPI (blue) was used to localize the nuclei; scale bar, 100 μm. (B) HE staining was used to detect scar density, and Masson and Sirius Red (SR) staining was used to indicate the variation in collagen synthesis *in vivo*; scale bar, 50 μm. (C) Statistical analysis of collagen synthesis with SR staining. (D) IHC staining of PCNA, tubulin and LC3B *in vivo*, and (E, F) the results of statistical analyses of the positive cell rates; scale bar, 60 μm; (G) Chemical structure of Tan IIA. Data are shown as the means ± standard deviations (SDs) from three independent samples; *P < 0.05 vs. control.

Tan IIA inhibited rabbit arthrofibrosis by regulating fibroblast proliferation, migration and autophagy in vivo

IHC staining was used to verify the relationship between fibroblast functions and Tan IIA treatment in knee arthrofibrosis. As noted in **Figure 1D**, the IHC results indicated that Tan IIA suppressed fibroblast proliferation and migration in a dose-dependent manner and increased cell autophagy. Compared with those in control group, the PCNA- and tubulin-positive rates in the 10 mg/mL Tan IIA treatment group respectively were decreased by 38% and 40% (**Figure 1E**), whereas, the LC3-positive rate in the 10 mg/mL Tan IIA treatment group was increased by 42% (**Figure 1F**). Considering this interesting phenomenon, we hypothesized that Tan IIA might suppress arthrofibrosis by regulating fibroblast autophagy, proliferation and migration.

Tan IIA restrained fibroblast proliferation in vitro

CCK-8 assays were used to detect the inhibitory effect of Tan IIA on fibroblast viability. The CCK-8 results showed that cell viability was decreased in a dose- and time-dependent manner and 20 μM Tan IIA induced approximately 50% growth inhibition at 48 h (**Figure 2A**). EdU analysis showed that EdU-positive fibroblasts decreased as the Tan IIA concentra-

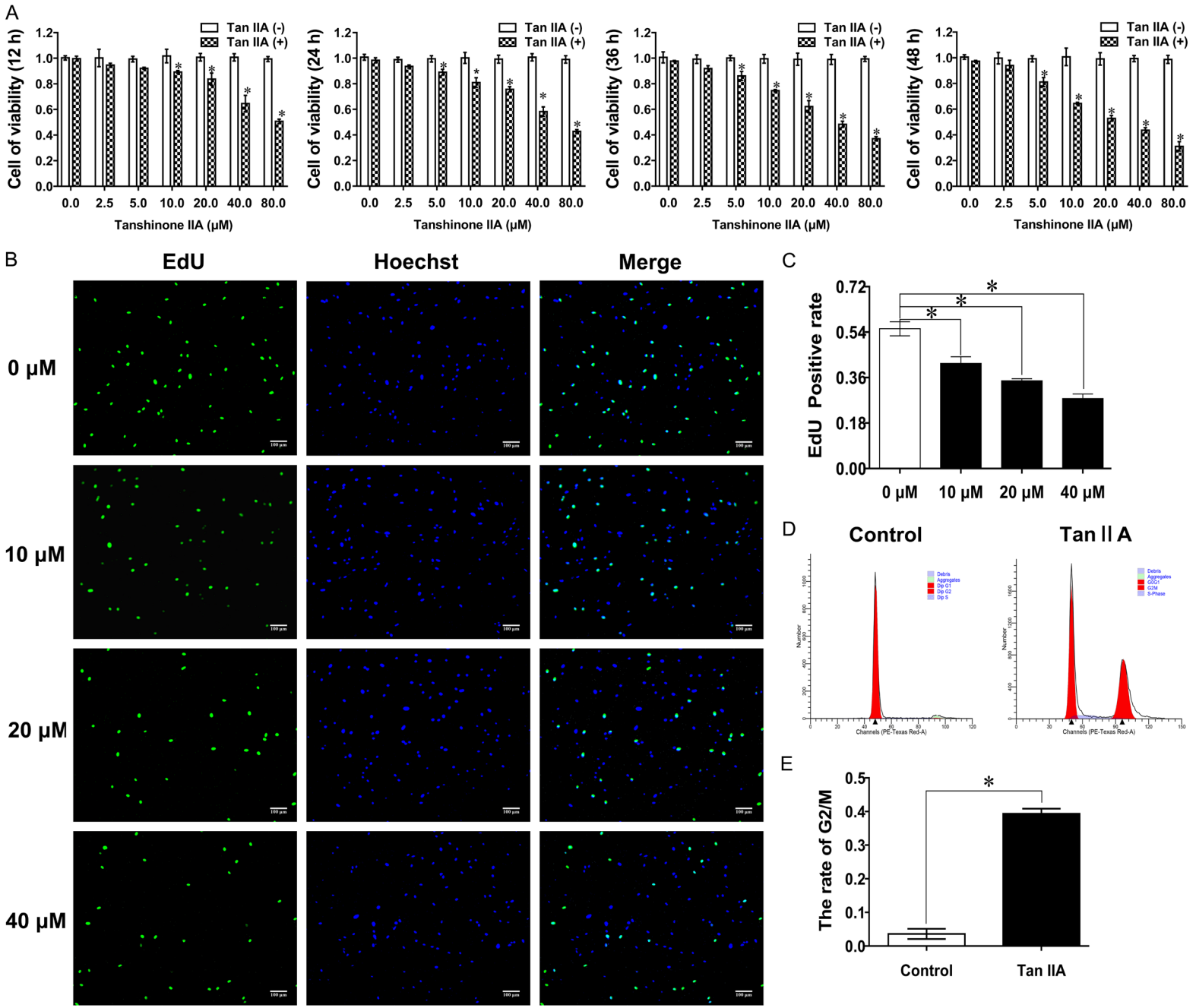
A
Cell of viability (12 h)
Cell of viability (24 h)
Cell of viability (36 h)
Cell of viability (48 h)
Tan IIA (-)
Tan IIA (+)
0.0 2.5 5.0 10.0 20.0 40.0 80.0
Tanshinone IIA (μM)
B
EdU
Hoechst
Merge
0 μM
10 μM
20 μM
40 μM
C
EdU Positive rate
0.00 0.18 0.36 0.54 0.72
0 μM 10 μM 20 μM 40 μM
D
Control
Tan II A
Channels (PE-Texas Red-A)
E
The rate of G2/M
0.0 0.1 0.2 0.3 0.4 0.5
Control
Tan IIA

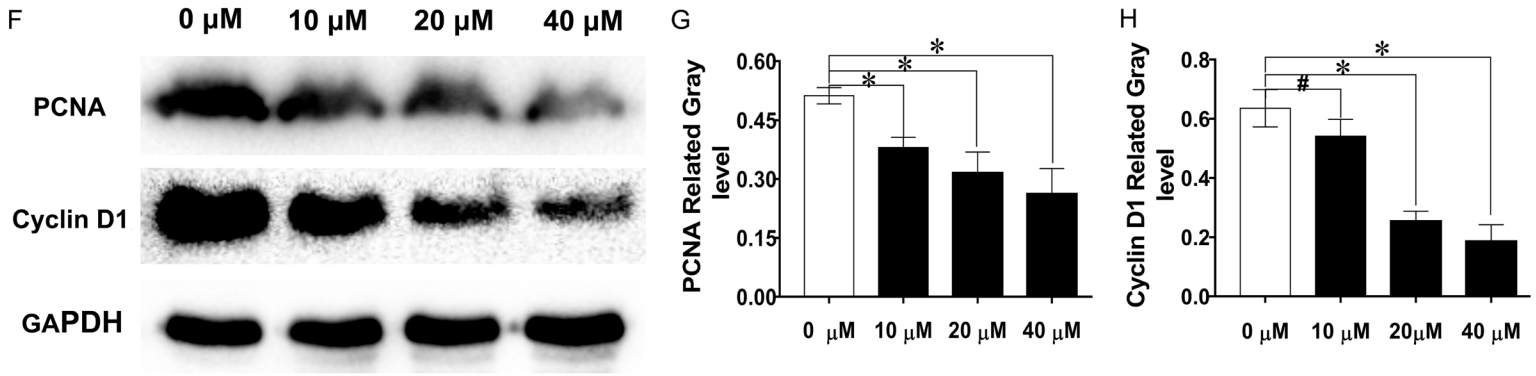

Figure 2. Tan IIA suppressed fibroblast proliferation. A. The inhibitory effects of Tan IIA treatment for 12, 24, 36, and 48 h against fibroblast viability were determined by CCK-8 assay. B, C. The rate of fibroblast proliferation after treatment with Tan IIA for 48 h was detected by EdU staining. D. Cell cycle analysis of fibroblasts treated with Tan IIA for 48 h. E. The proportion of fibroblasts at G2/M phase was calculated. F. Western blot was used to determine the expression of PCNA and cyclin D1. G, H. PCNA and cyclin D1 expression was quantified by normalization to GAPDH expression. The data are shown as the means ± SDs from three independent experiments; *P < 0.05 vs. control.

tion increased. Compared with the 0 μM group, the positive rate decreased 27% in the 40 μM group (**Figure 2B**, **2C**). As shown in **Figure 2D**, Tan IIA suppressed fibroblast proliferation by arresting cells in G2/M phase. PCNA and cyclin D1 protein expression was used to demonstrate alterations in cell proliferation. The results showed that the expression of the proliferation-related proteins was also suppressed with Tan IIA intervention (**Figure 2F-H**). The above results confirmed that Tan IIA could restrain fibroblast proliferation.

Tan IIA suppressed fibroblast migration in vitro

Wound closure, Transwell and cytoskeleton protein IF assays were used to detect the inhibitory effect of Tan IIA on fibroblast migration. **Figure 3A** demonstrates that fibroblast migration was suppressed, and cellular morphology was also altered with Tan IIA treatment. The number of migrated cells attached to the bottom membrane after treatment with 20 μM and 40 μM Tan IIA were reduced 46% and 66%, respectively, compared with the 0 μM group (**Figure 3B**). Most cells exhibited an irregular polygonal shape rather than a typical spindle shape after treatment with 40 μM Tan IIA for 48 h (**Figure 3A**). Wound closure assay results showed that Tan IIA inhibited fibroblast migration in a dose-dependent manner (**Figure 3C**). Compared with that in the 0 μM group, wound closure ability was reduced approximately 40% after treatment with 40 μM Tan IIA for 36 h (**Figure 3D**). Furthermore, as shown in **Figure 3E**, tubulin fibres were no longer straight, and vinculin exhibited a dispersed pattern of expression in the cytoplasm after treatment with Tan IIA, especially in the medium- and high-concentration groups. Additionally, the western blot results showed that the levels of migration-related proteins were reduced with increasing Tan IIA concentration (**Figure 3F-H**). All these results indicated that Tan IIA suppressed fibroblast migration *in vitro*.

Tan IIA stimulated autophagy in fibroblasts, and the effect was partially reversed after combined treatment with 3-MA

TEM, IF-LC3 and western blot were used to verify that Tan IIA could stimulate autophagy in fibroblast *in vitro*. TEM showed that many double-membrane vesicles containing various organelles and cytoplasm were induced in the Tan IIA group (**Figure 4B**). IF-LC3 is a reliable method to detect LC3. As shown in **Figure 4A**, fluorescent LC3 puncta continuously increased with increasing Tan IIA concentration. Additionally, the autophagy-related proteins LC3, p62, Beclin 1 and Atg5 were detected by western blot, and their expression levels were found to decrease in a Tan IIA dose-dependent manner (**Figure 4C-G**). These data indicated that Tan IIA could stimulate autophagy in fibroblasts.

As above results indicated that Tan IIA regulates fibroblast proliferation, migration and autophagy. We hypothesized that Tan IIA, as an external stimulus, could curb cell proliferation and migration by inducing fibroblast autophagy. To verify this hypothesis, 3-MA, a classical autophagy inhibitor, was used to inhibit the autophagy induced by Tan IIA. The IF-LC3 results revealed that Tan IIA could induce fibroblast autophagy, and the number of LC3 fluorescence puncta was decreased after combined treatment with 3-MA (**Figure 4H**). Moreover, western blot indicated that the altered expression of the autophagy-related proteins p62, Beclin-1, Atg5 and LC-3 induced by Tan IIA was partially reversed after combined treatment with 3-MA (**Figure 4I-M**). These results demonstrated that fibroblast autophagy induced by Tan IIA could be partially inhibited by combined treatment with 3-MA.

Tan IIA-mediated attenuation of fibroblast proliferation might occur via autophagy induction

The EdU assay data suggested that the proportion of EdU-labelled positive fibroblasts was increased by 10% after combined treatment with 3-MA compared with that in the Tan IIA group (**Figure 5A**, **5B**). In addition, as presented in **Figure 5C**, **5D**, the rate of cells at G2 phase was reduced after combined treatment with 3-MA compared with that upon Tan IIA treatment alone. Moreover, western blot showed that the inhibitory effect of Tan IIA on PCNA and cyclin D1 expression was also reversed with combined treatment with 3-MA (**Figure 5E-G**). All the results indicated that the inhibitory effect of Tan IIA on fibroblast proliferation could be reversed by inhibiting Tan IIA-induced autophagy.

Tan IIA-mediated suppression of fibroblast migration might occur via autophagy induction

To explore the relationship between fibroblast migration and autophagy induced by Tan IIA,

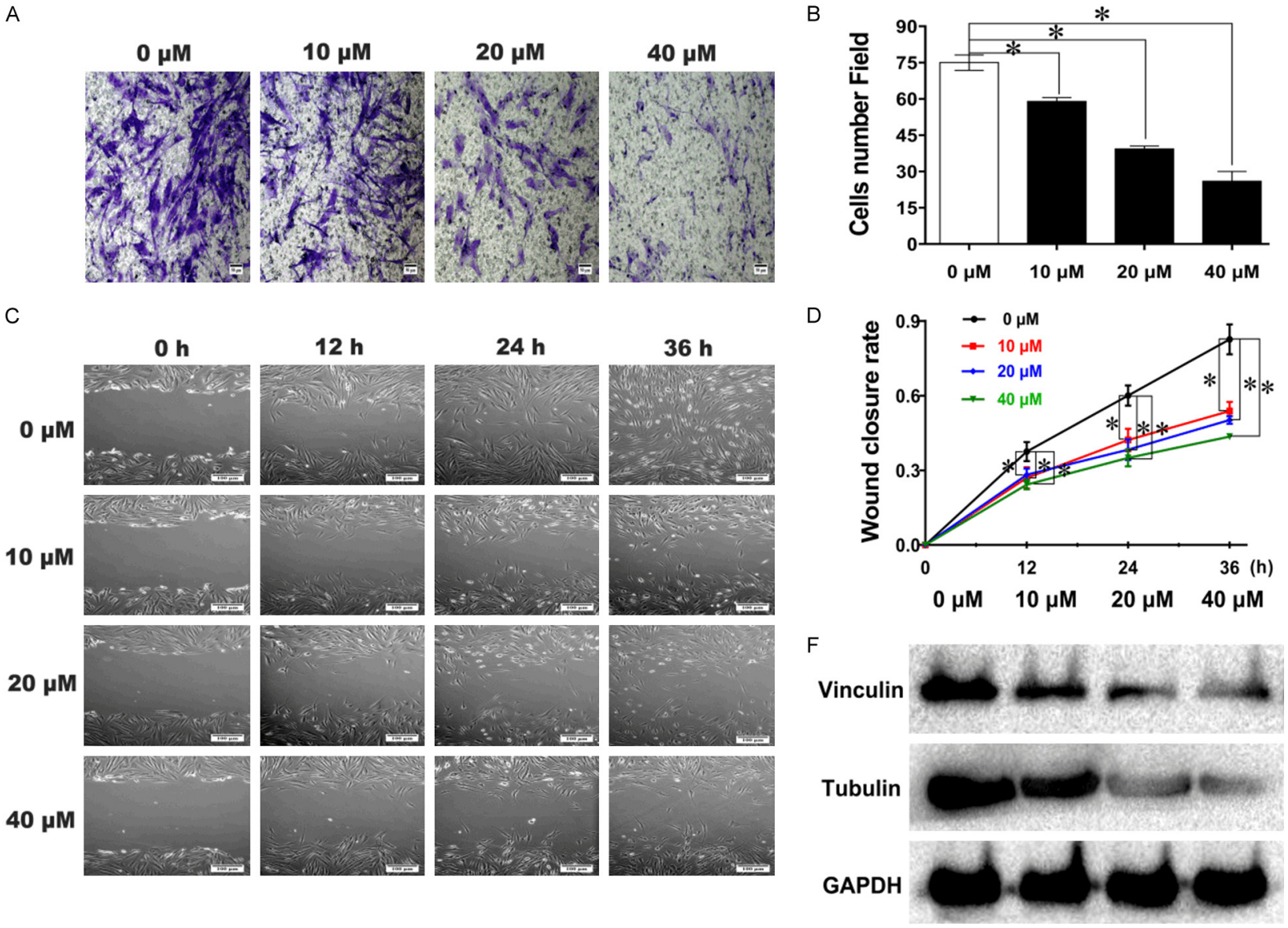
A
0 μM
10 μM
20 μM
40 μM
B
Cells number Field
90
75
60
45
30
15
0
0 μM
10 μM
20 μM
40 μM
C
0 h
12 h
24 h
36 h
0 μM
10 μM
20 μM
40 μM
D
Wound closure rate
0.9
0.6
0.3
0.0
0 μM
10 μM
20 μM
40 μM
0
12
24
36 (h)
0 μM
10 μM
20 μM
40 μM
F
Vinculin
Tubulin
GAPDH

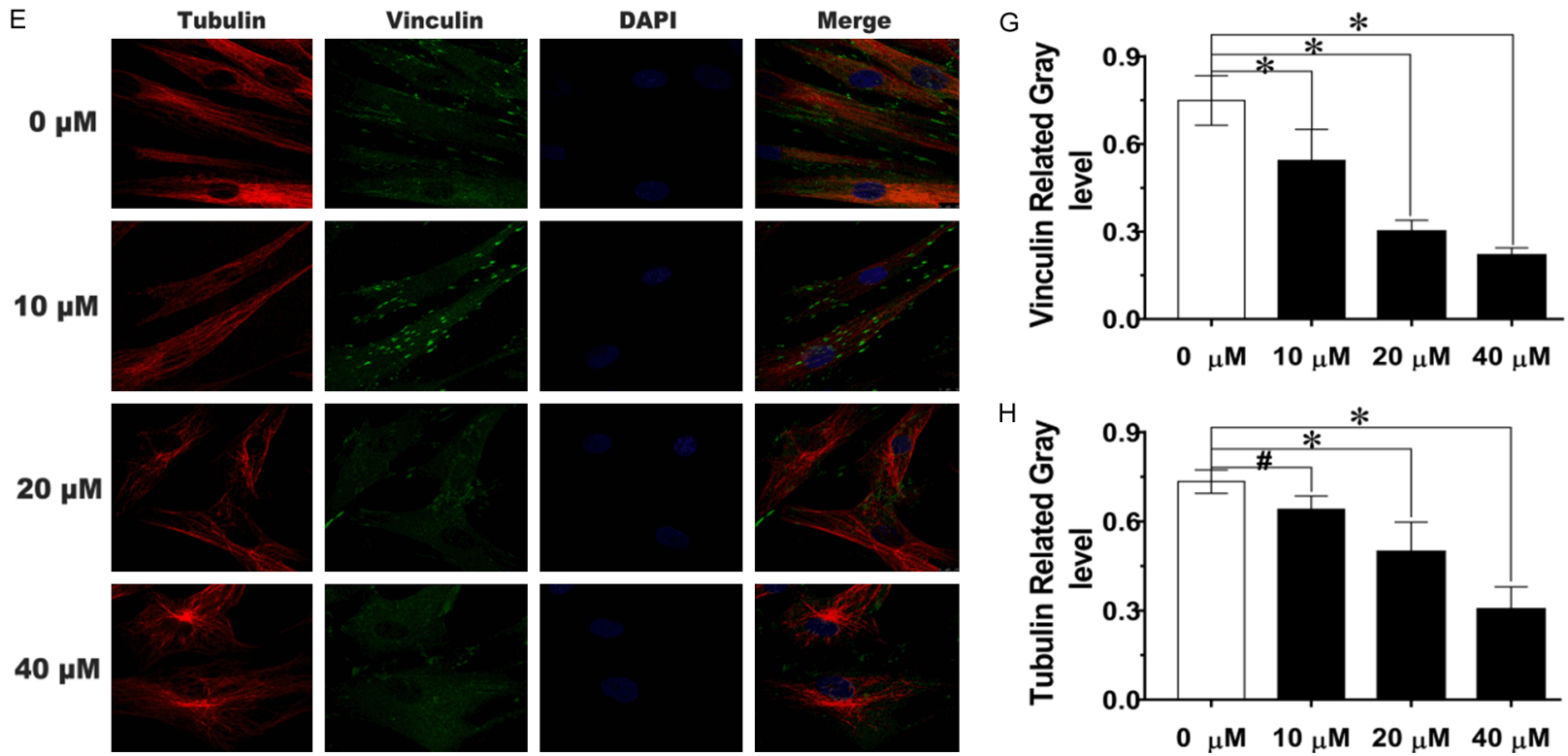

Figure 3. Tan IIA inhibited fibroblast migration. A, C. The repressive effects of Tan IIA against the migration of fibroblasts were visualized using Transwell and Scratch wound assays; scale bars, 50 and 100 μm. B. The number of migrated fibroblasts that had attached to the bottom membrane after Tan IIA treatment for 48 h. D. Wound closure rate of cells treated with Tan IIA for 0, 12, 24, or 36 h. E. Confocal images of the cytoskeleton proteins tubulin and vinculin after treatment with Tan IIA for 48 h; scale bar, 10 μm. F. The expression of tubulin and vinculin was analysed by western blot. G, H. Tubulin and vinculin expression was quantified by normalization to GAPDH expression. Data are shown as the means ± SDs from three independent experiments; *P < 0.05 vs. control.

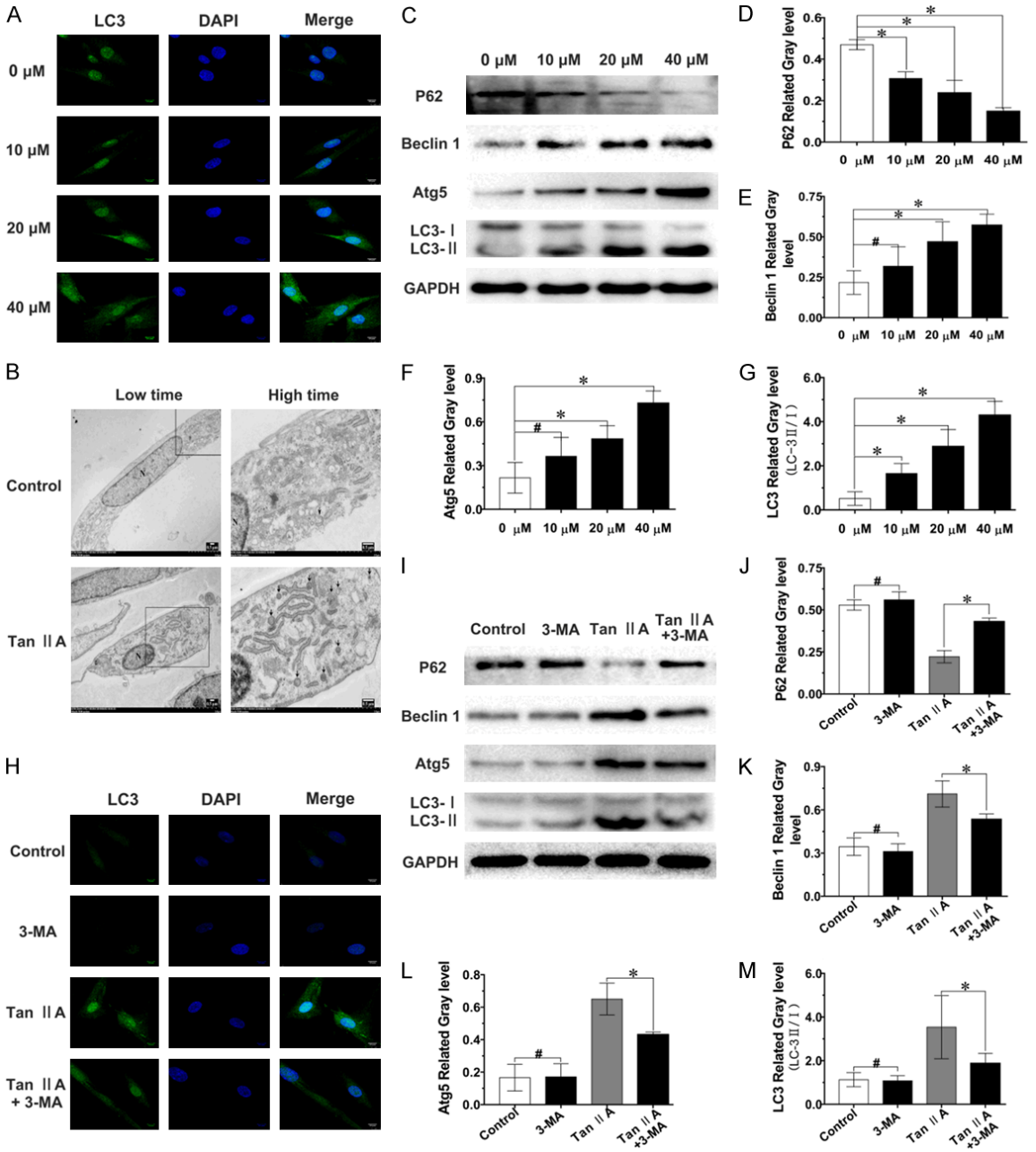

Figure 4. Tan IIA induced fibroblast autophagy, which was partially suppressed by 3-MA. A. Confocal images of LC3; scale bar, 10 μm. B. TEM images of a fibroblast autophagosome (black arrow) induced by Tan IIA treatment for 48 h. N, nucleus; scale bar, 0.5 μm. C-G. Expression levels of p62, Beclin 1, Atg5 and LC3-II/I were determined by western blot and quantified by normalization to GAPDH levels. H. Confocal images of LC3 after treatment with 3-MA and/or Tan IIA; scale bar, 10 μm. I-M. The expression of p62, Beclin-1, Atg5 and LC3-II/I was analysed by western blot, and the expression of p62, Beclin 1, Atg5 was quantified by normalization to GAPDH expression, the levels of LC3-II/I ratio is shown. Data are shown as the means ± SDs from three independent experiments; *P < 0.05; #P > 0.05.

Wound closure, Transwell and IF assays were performed after combined treatment with Tan IIA and 3-MA. Transwell and IF analyses showed that the fibroblast morphology was altered after treatment with 40 μM Tan IIA compared to that of the control, but the changes in cell morphology were partially reversed after combination treatment with 3-MA (**Figure 6A**, **6E**). The results of the Wound closure assay were similar, and the ability of cells to close the cellular

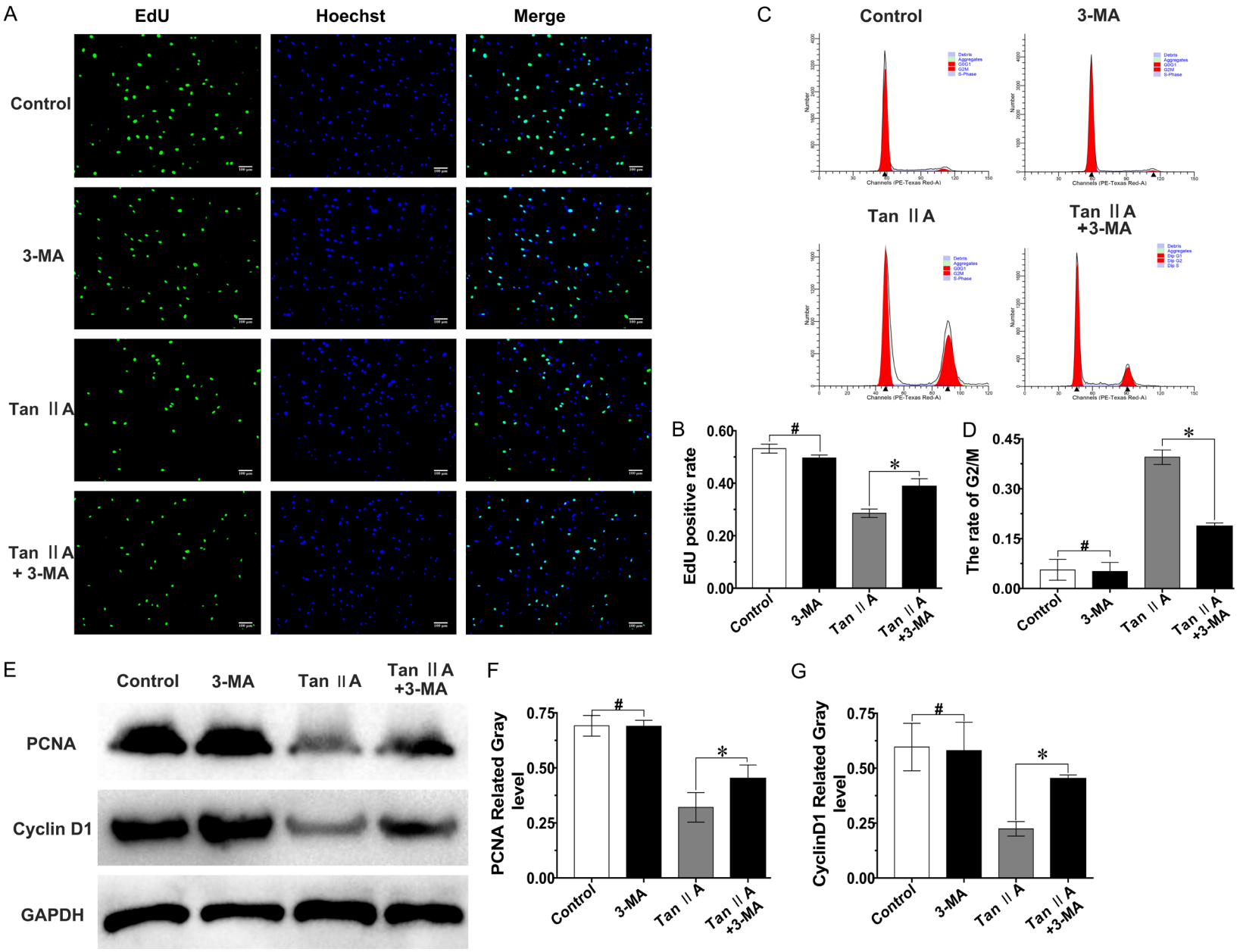
A
EdU
Hoechst
Merge
Control
3-MA
Tan ⅡA
Tan ⅡA + 3-MA
B
EdU positive rate
0.60
0.40
0.20
0.00
#
*
Control
3-MA
Tan ⅡA
Tan ⅡA +3-MA
C
Control
3-MA
Tan ⅡA
Tan ⅡA +3-MA
Debris
Aggregates
G0/G1
G2M
S-Phase
Number
Channels (PE-Texas Red-A)
D
The rate of G2/M
0.45
0.30
0.15
0.00
#
*
Control
3-MA
Tan ⅡA
Tan ⅡA +3-MA
E
Control
3-MA
Tan ⅡA
Tan ⅡA +3-MA
PCNA
Cyclin D1
GAPDH
F
PCNA Related Gray level
0.75
0.50
0.25
0.00
#
*
Control
3-MA
Tan ⅡA
Tan ⅡA +3-MA
G
CyclinD1 Related Gray level
0.75
0.50
0.25
0.00
#
*
Control
3-MA
Tan ⅡA
Tan ⅡA +3-MA

Figure 5. The inhibitory effect of Tan IIA against fibroblast proliferation could be partially reversed with 3-MA. A. Fluorescence microscopy images of EdU-positive (green) fibroblasts after treatment with 3-MA and/or Tan IIA for 48 h. Merged images showed overlap of the nucleus (blue); magnification, ×100; scale bar, 10 μm. B. Proportion of EdU-positive cells. C. Cell cycle analysis of fibroblasts after treatment with 3-MA and/or Tan IIA for 48 h. D. Proportion of fibroblasts at G2/M phase. E-G. PCNA and cyclin D1 expression was assessed by western blot and quantified by normalization to GAPDH expression. Data are shown as the means ± SDs from three independent experiments; *P < 0.05; #P > 0.05.

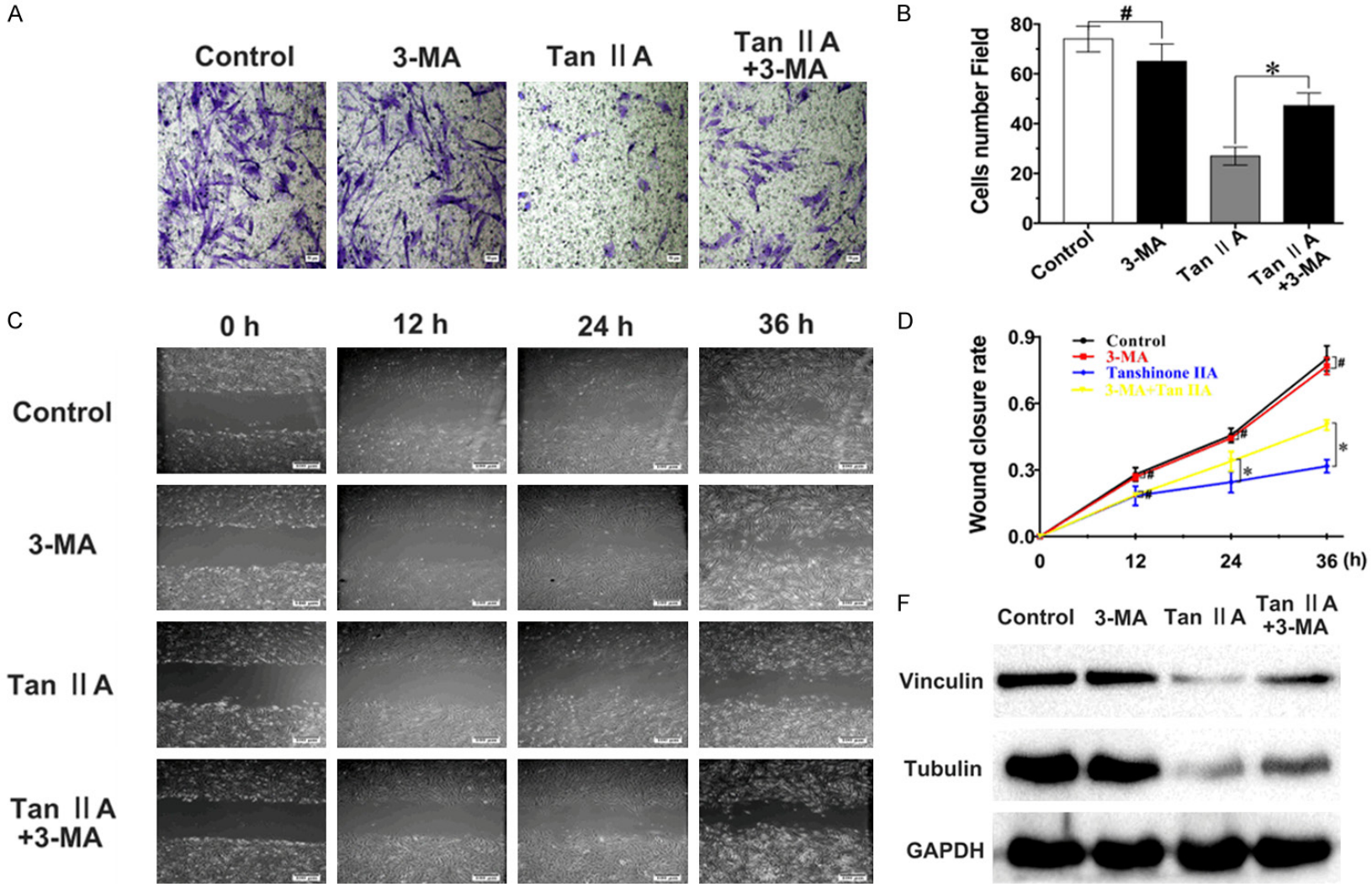

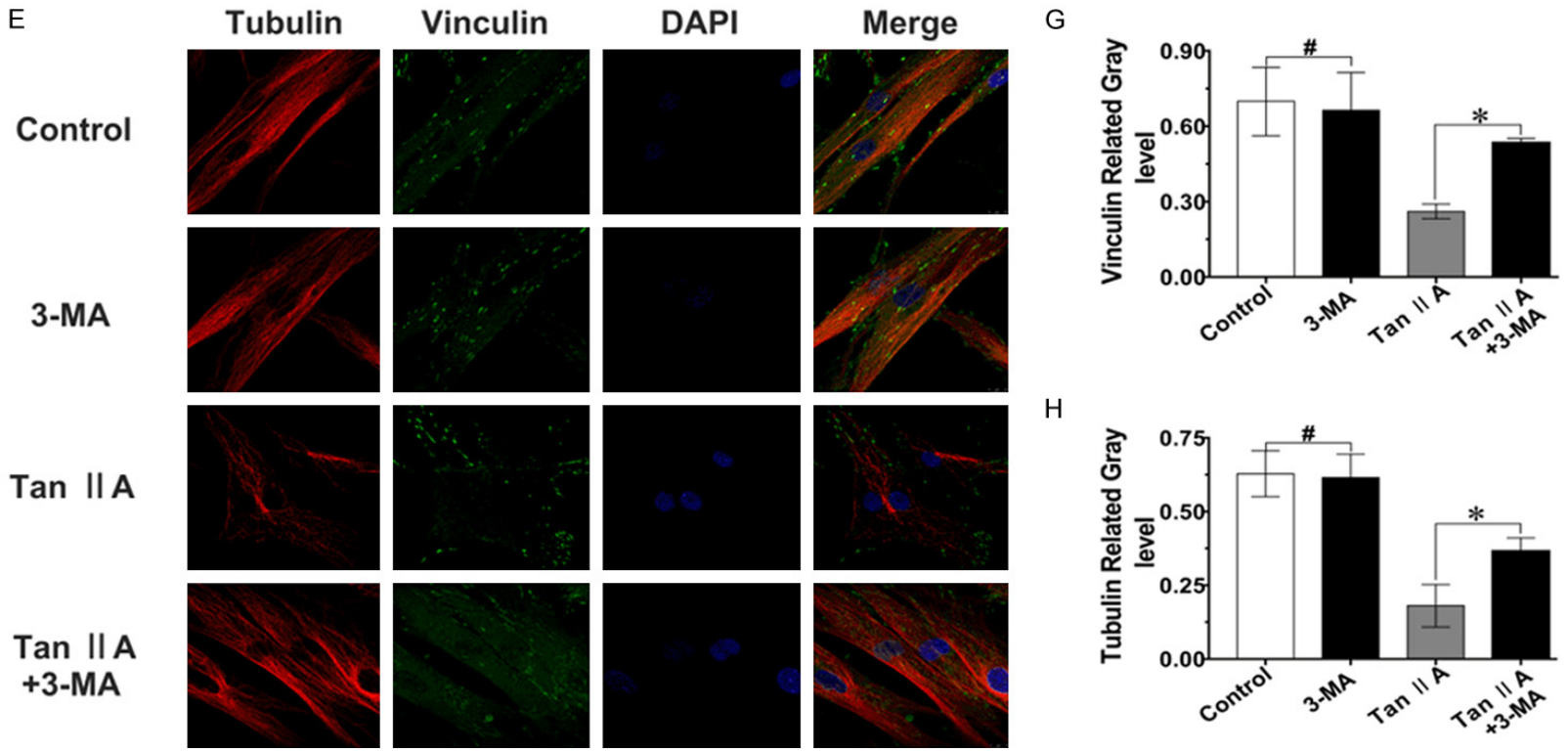

Figure 6. The suppressive effect of Tan IIA against fibroblast migration could be partially reversed with 3-MA. A, C. The inhibitory effects of Tan IIA against migration in fibroblasts were visualized with Transwell and Scratch wound experiments; scale bars, 50 and 100 μm. B. The number of migrated fibroblasts that attached to the bottom membrane after 3-MA and/or Tan IIA treatment for 48 h. D. Wound closure rate of cells treated with 3-MA and/or Tan IIA for 0, 12, 24, or 36 h. E. Confocal images of the cytoskeleton proteins tubulin and vinculin after treatment with 3-MA and/or Tan IIA for 48 h; scale bar, 10 μm. F-H. Tubulin and vinculin protein expression was confirmed by western blot and quantified by normalization to GAPDH expression. Data are shown as the means ± SDs of three independent experiments; *$P < 0.05$; #$P > 0.05$.

wound was increased by approximately 20% at 36 h following combined treatment with Tan IIA and 3-MA compared to treatment with Tan IIA alone (**Figure 6C**, **6D**). Moreover, the repressive effect of Tan IIA on the expression of migration-related proteins (vinculin and tubulin) was relieved with combination 3-MA treatment (**Figure 6F-H**). These results indicated that the inhibitory impact of Tan IIA on fibroblast migration could be alleviated by suppressing Tan IIA-induced autophagy.

Tan IIA inhibited fibroblast proliferation and migration by regulating autophagy through the PI3K and AMPK/mTOR pathways

Western blot was used to detect the pathways involved in Tan IIA-mediated regulation of fibroblast migration, proliferation and autophagy. Various concentrations of Tan IIA were used to treat fibroblasts for 48 h. The assay results showed that the expression levels of p-PI3K, p-AKT and p-mTOR were reduced, while that of p-AMPK was increased in a dose-dependent manner after treatment with Tan IIA (**Figure 7A-F**). These results suggested that Tan IIA might regulate fibroblast function through the PI3K and AMPK/mTOR signaling pathways.

As shown in **Figure 7G-K**, the alteration of pathways-related proteins induced by Tan IIA could be reversed to a certain degree after combined treatment with 3-MA for 48 h. We observed the restored expression of p-PI3K/p-AKT/p-mTOR after combined Tan IIA and 3-MA treatment; meanwhile, p-AMPK expression was reduced after combined treatment compared with that upon Tan IIA treatment alone. Together, the above results suggested that Tan IIA-mediated regulation of fibroblast autophagy to suppress proliferation and migration may be mediated through the PI3K and AMPK/mTOR signaling pathways.

Discussion

In the present study, we verified that Tan IIA could inhibit post-surgery arthrofibrosis *in vivo*. This study indicates that the induction of fibroblast autophagy increased the inhibitory effect of Tan IIA against fibroblast proliferation and migration, demonstrating that autophagy induced by Tan IIA may play a key role in Tan IIA-mediated suppression of post-surgery arthrofibrosis.

As previously stated, cell proliferation and migration play a role in the formation of post-surgery arthrofibrosis. Interestingly, Tan IIA possesses anti-inflammatory, anti-migration and anti-proliferation functions [15, 23]. In addition, Tan IIA could prevent LPS-and high glucose-induced cardiac fibrosis in mice [24].

Considering the above evidence, the notion that Tan IIA can potentially inhibit postsurgery arthrofibrosis is more convincing. Fortunately, the present study results demonstrated that arthrofibrosis was alleviated after the topical administration of Tan IIA *in vivo*.

Collagen is one of the most important components of the ECM and promotes cell survival and migration [25]. Fibroblasts, which are the primary collagen-producing cells in periarticular tissues, generate excess collagen deposits in periarticular tissues, leading to periarticular fibrogenesis [26].

In this study, Masson staining showed that collagen deposition was alleviated after treatment with Tan IIA. Moreover, type I and III collagens, the major collagen components, were inhibited with Tan IIA treatment in a dose-dependent manner, as shown by SR staining. Meanwhile, previous clinical studies have shown that collagen I and III are the major components of collagen synthesis in the surgical area [27]. Here, the results indicated that the rabbit model could effectively imitate post-operative arthrofibrosis.

Previous studies have reported that excessively proliferating fibroblasts will migrate to the area after surgery, leading to excessive collagen deposition and ultimately resulting in arthrofibrosis formation [4]. Interestingly, the IHC results showed that Tan IIA suppressed expression of the proliferation- and migration-related proteins PCNA and tubulin. Mounting evidence indicates that autophagy plays a role in fibrosis, and a recent study found that autophagy may be a crucial therapeutic target in fibrotic disease [28]. Interestingly, the IHC results showed that the expression of LC3B in the area was increased in a dose-dependent manner. Both IHC and histological analyses indicated that fibroblast autophagy induced by

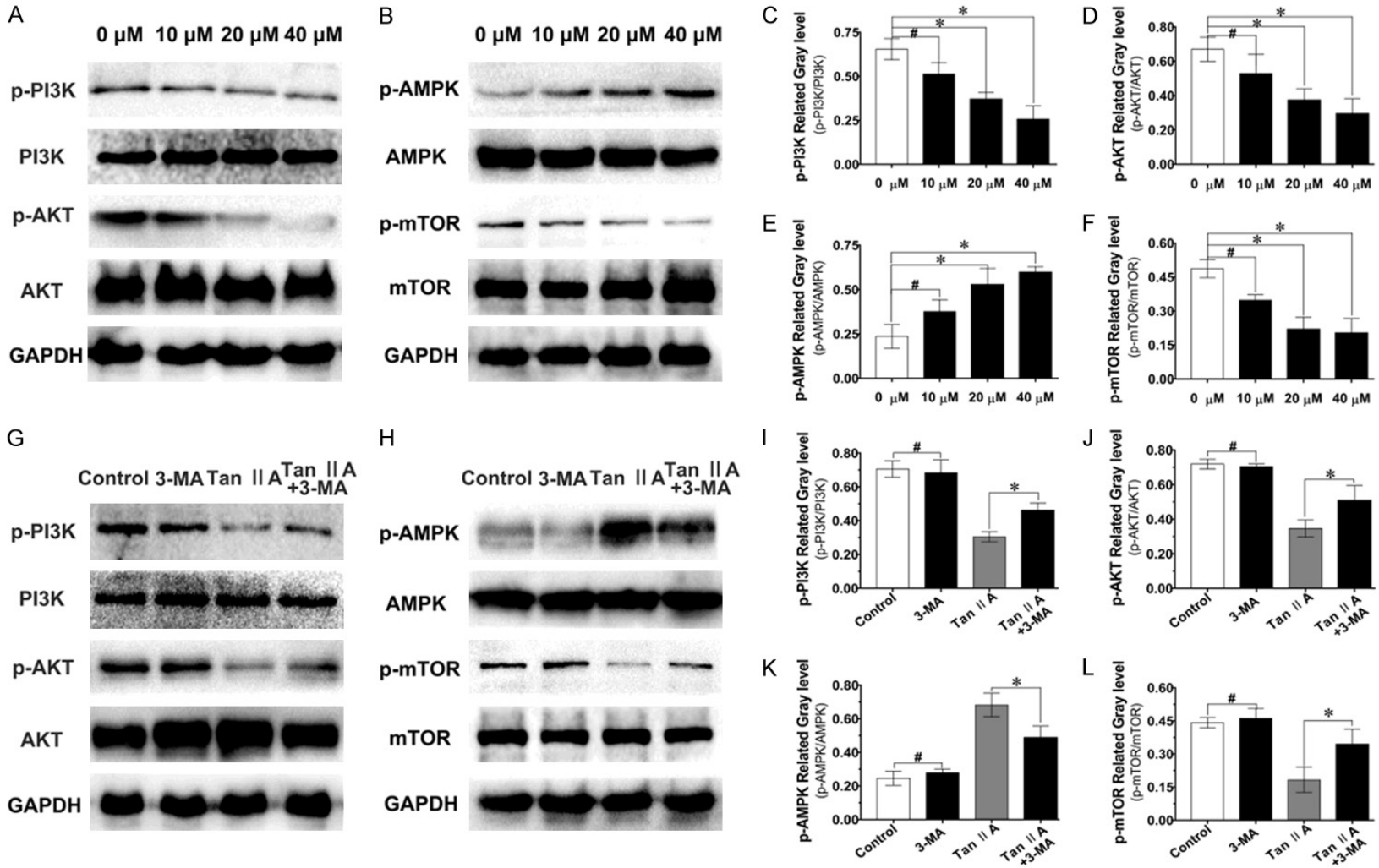

Figure 7. Tan IIA-inhibited fibroblast proliferation and migration might occur through autophagy regulation mediated by the PI3K/AMPK-mTOR signaling pathway. A, B. After treatment with Tan IIA at various concentrations, the expression of p-PI3K, PI3K, p-AKT, AKT, p-AMPK, AMPK, p-mTOR, and mTOR was verify by western blot. G, H. After treatment with Tan IIA or Tan IIA and 3-MA for 48 h, the expression of p-PI3K, PI3K, p-AKT, AKT, p-AMPK, AMPK, p-mTOR, and mTOR was analysed by western blot. GAPDH was used as the endogenous control. C-F and I-L. The relative expression of p-PI3K, p-Akt, p-AMPK, p-mTOR was quantified by normalization to PI3K, Akt, AMPK and mTOR, respectively. GAPDH was used as the endogenous control. Data are shown as the means ± SDs of three independent samples; *$P < 0.05$, #$P > 0.05$.

Tan IIA plays a negative role in regulating arthrofibrosis.

Autophagy, a 'self-digestion' process that aims to reuse cellular components to adapt to starvation and stress, participates in many aspects of biology [29]. Indeed, studies have demonstrated that autophagy is a potential target in preventing fibrosis [28, 30]. Fibroblast proliferation and migration play a crucial role in arthrofibrosis. However, the mechanism of autophagy in fibrosis is complicated. One study showed that excessive autophagy stimulated lung-derived fibroblast proliferation and migration and aggravated pulmonary fibrosis [31]. Another study reached the opposite conclusion, reporting that pulmonary fibrosis induced by crystalline silica could be attenuated by stimulating alveolar macrophage autophagy [32]. In the present study, the IHC results showed that Tan IIA could induce autophagy *in vivo* in the cells in the exposed area.

The results of TEM confirmed that fibroblast autophagy was induced with Tan IIA treatment *in vitor*. Moreover, the hypothesis that Tan IIA could induce fibroblasts autophagy was verified by IF-LC3 and western blot. However, conversely, Tan IIA was reported to inhibit autophagy in vascular smooth muscle cells by inducing Angiotensin II [33]. We speculate that this contradiction may be due to the dual roles of autophagy in cell protection and pathological disease progression.

The EdU assay results indicated that Tan IIA restrained fibroblast proliferation. The proliferation of somatic cells during the mitotic process is determined by progression through the cell cycle [34]. In the present study, fibroblasts were arrested at G2/M phase after Tan IIA treatment, which is similar to the findings of another study [35]. Moreover, fibroblast migration was gradually restrained with increasing Tan IIA concentration in Transwell and Wound closure assays. The microtubule proteins tubulin and vinculin, which are important components of the cytoskeleton, are crucial for fibroblast migration [36]. One study found that Tan IIA could alleviate cardiac fibrosis by inhibiting the expression of β-tubulin [37]. The IF-C results for tubulin and vinculin indicated that Tan IIA could decrease fibroblast migration by disturbing microtubule stabilization. Interestingly, a recent study showed that Tan IIA could alleviate rheumatoid arthritis by inhibiting fibroblast-like synoviocyte proliferation and migration [38].

The *in vitro* results suggested that Tan IIA could inhibit fibroblast proliferation and migration and induce autophagy. When fibroblasts were treated with a combination of Tan IIA and 3-MA, the IF-LC3, EdU and Transwell assays results suggested that fibroblast autophagy was suppressed, and the suppression of fibroblast proliferation and migration induced by Tan IIA was partially reversed. Moreover, fibroblast proliferation and migration were not significantly altered upon 3-MA administration compared with those in the control group, indicating that the ability of Tan IIA to restrain fibroblast proliferation and migration might occur through autophagy induction.

mTOR, a negative regulator of autophagy, is the best characterized autophagy hub protein in cells [39]. Mounting evidence suggests that mTOR is an important potential therapeutic target in diseases in which autophagy is involved [40]. Moreover, mTOR plays a role in fibrosis diseases by regulating cell autophagy [41]. In addition, Tan IIA was demonstrated to induce autophagy in U937 cells through regulation of the PI3K/AKT/mTOR signaling pathway [17]. In this study, we also revealed that Tan IIA induced fibroblast autophagy by downregulating p-PI3K/p-AKT/p-mTOR and upregulating p-AMPK. Moreover, another study indicated that Tan IIA could stimulate autophagy in H9C2 cells via activation of the AMPK/mTOR pathway [18].

Interestingly, in fibroblasts that were exposed to combined intervention with Tan IIA and 3-MA, the expression levels of p-PI3K/p-AKT, p-AMPK and p-mTOR were all partially reversed compared with those in fibroblasts treated with Tan IIA alone. These results illustrate that Tan IIA-induced fibroblast autophagy might be mediated through modulation of the PI3K/AMPK-mTOR pathways. Interestingly, Tan IIA could alleviate dermal fibrosis induced by bleomycin by preventing the activation of mTOR signaling [42]. Thus, Tan IIA was proposed to mitigate post-operative arthrofibrosis through autophagy regulation mediated by the mTOR signaling pathway.

However, some limitations exist. First, in the present study, only the autophagy inhibitor 3-MA was added, and the exploration of the signaling pathway was insufficient. In the next study, a signaling pathway inhibitor will be used. Second, a positive autophagy drug control was not included as a reference. In further studies, a reference drug, such as rapamycin, will be used. Third there is no experiment about the effect of Tan IIA on other normal articular cell types, and the effects of Tan IIA on other cells will be assessed in future studies. Fourth, the inflammatory reaction and myofibroblast-related chemokine-induced myofibroblast migration are known to play key roles in the occurrence of arthrofibrosis; however, these related assays were not involved in this study. The inhibitory effect of Tan IIA on cells inflammatory reaction and myofibroblast-related chemokine-induced myofibroblasts migration will be assessed in future studies. Finally, the dose used for topical application was not optimized. In further experiments, more drug concentrations will be explored.

Conclusion

In conclusion, the results demonstrated that the topical application of Tan IIA attenuated post-surgery arthrofibrosis, potentially mediated through the induction of fibroblast autophagy, which regulates proliferation and migration via the PI3K and AMPK-mTOR signaling pathways.

Acknowledgements

The study was funded by the National Natural Science Foundation of China (grant No. 81772332), Jiangsu Provincial Medical Innovation Team (grants No. # CXTDB2017004), and Six Talent Peaks Project Jiangsu Province (No. 2015-WSN-110).

Disclosure of conflict of interest

None.

Address correspondence to: Drs. Jingcheng Wang and Lianqi Yan, Department of Orthopedics, Clinical Medical College of Yangzhou University, 98 Nantong Road, Yangzhou 225001, Jiangsu, China. Tel: +86-18051063952; Fax: +86-0514-87937406; E-mail: jingchengwyz@163.com (JCW); Tel: +86-18051060191; Fax: +86-0514-87937406; E-mail: yanlianqi@126.com (LQY)

References

[1] Yercan HS, Sugun TS, Bussiere C, Ait Si Selmi T, Davies A and Neyret P. Stiffness after total knee arthroplasty: prevalence, management and outcomes. Knee 2006; 13: 111-117.

[2] McAlister I and Sems SA. Arthrofibrosis after periarticular fracture fixation. Orthop Clin North Am 2016; 47: 345-355.

[3] Rushdi I, Sharifudin S and Shukur A. Arthrofibrosis following anterior cruciate ligament reconstruction. Malays Orthop J 2019; 13: 34-38.

[4] Bayram B, Limberg AK, Salib CG, Bettencourt JW, Trousdale WH, Lewallen EA, Reina N, Paradise CR, Thaler R, Morrey ME, Sanchez-Sotelo J, Berry DJ, van Wijnen AJ and Abdel MP. Molecular pathology of human knee arthrofibrosis defined by RNA sequencing. Genomics 2020; 112: 2703-2712.

[5] Li X, Chen S, Yan L, Wang J and Pei M. Prospective application of stem cells to prevent post-operative skeletal fibrosis. J Orthop Res 2019; 37: 1236-1245.

[6] Levine B and Kroemer G. Biological functions of autophagy genes: a disease perspective. Cell 2019; 176: 11-42.

[7] Mizushima N, Levine B, Cuervo AM and Klionsky DJ. Autophagy fights disease through cellular self-digestion. Nature 2008; 451: 1069-1075.

[8] Zhao XC, Livingston MJ, Liang XL and Dong Z. Cell apoptosis and autophagy in renal fibrosis. Adv Exp Med Biol 2019; 1165: 557-584.

[9] Wan Q, Chen H, Xiong G, Jiao R, Liu Y, Li X, Sun Y, Wang J and Yan L. Artesunate protects against surgery-induced knee arthrofibrosis by activating Beclin-1-mediated autophagy via inhibition of mTOR signaling. Eur J Pharmacol 2019; 854: 149-158.

[10] Yu JS and Cui W. Proliferation, survival and metabolism: the role of PI3K/AKT/mTOR signalling in pluripotency and cell fate determination. Development 2016; 143: 3050-3060.

[11] Luo M, Liu Q, He M, Yu Z, Pi R, Li M, Yang X, Wang S and Liu A. Gartanin induces cell cycle arrest and autophagy and suppresses migration involving PI3K/Akt/mTOR and MAPK signalling pathway in human glioma cells. J Cell Mol Med 2017; 21: 46-57.

[12] Gao L, Lv G, Li R, Liu WT, Zong C, Ye F, Li XY, Yang X, Jiang JH, Hou XJ, Jing YY, Han ZP and Wei LX. Glycochenodeoxycholate promotes hepatocellular carcinoma invasion and migration by AMPK/mTOR dependent autophagy activation. Cancer Lett 2019; 454: 215-223.

[13] Garza-Lombo C, Schroder A, Reyes-Reyes EM and Franco R. mTOR/AMPK signaling in the brain: cell metabolism, proteostasis and survival. Curr Opin Toxicol 2018; 8: 102-110.

[14] Lv XX, Liu SS and Hu ZW. Autophagy-inducing natural compounds: a treasure resource for developing therapeutics against tissue fibrosis. J Asian Nat Prod Res 2017; 19: 101-108.
[15] Chen Z, Gao X, Jiao Y, Qiu Y, Wang A, Yu M, Che F, Li S, Liu J, Li J, Zhang H, Yu C, Li G, Gao Y, Pan L, Sun W, Guo J, Cao B, Zhu Y and Xu H. Tanshinone IIA exerts anti-inflammatory and immune-regulating effects on vulnerable atherosclerotic plaque partially via the TLR4/MyD88/NF-kappaB signal pathway. Front Pharmacol 2019; 10: 850.
[16] Cao L, Huang B, Fu X, Yang J, Lin Y and Lin F. Effects of tanshinone IIA on the regulation of renal proximal tubular fibrosis. Mol Med Rep 2017; 15: 4247-4252.
[17] Zhang Y, Geng Y, He J, Wu D, Zhang T, Xue L, Zhang L and He A. Tanshinone IIA induces apoptosis and autophagy in acute monocytic leukemia via downregulation of PI3K/Akt pathway. Am J Transl Res 2019; 11: 2995-3006.
[18] Zhang X, Wang Q, Wang X, Chen X, Shao M, Zhang Q, Guo D, Wu Y, Li C, Wang W and Wang Y. Tanshinone IIA protects against heart failure post-myocardial infarction via AMPKs/mTOR-dependent autophagy pathway. Biomed Pharmacother 2019; 112: 108599.
[19] Liang L, Xie Q, Li WH, Zeng Z, Huang ZR and Li DL. The effect of tanshinone II A on the transmembrance action potential of myocardial cells in LQT2 rabbit models. Sichuan Da Xue Xue Bao Yi Xue Ban 2013; 44: 744-746.
[20] Liang Y, Sun Y, Li X, Yan L, Wang J, Hu J, Yu H, Xiao H, Chen H, Sun Z, Cai J, Feng X, Xiong C and He J. The optimal concentration of topical hydroxycamptothecin in preventing intraarticular scar adhesion. Sci Rep 2014; 4: 4621.
[21] Zhang Y, Feng Y, Justus CR, Jiang W, Li Z, Lu JQ, Brock RS, McPeek MK, Weidner DA, Yang LV and Hu XH. Comparative study of 3D morphology and functions on genetically engineered mouse melanoma cells. Integr Biol (Camb) 2012; 4: 1428-1436.
[22] Nadal M and Gold SE. Assessment of autophagosome formation by transmission electron microscopy. Methods Mol Biol 2012; 835: 481-489.
[23] Chen Y, Wu X, Yu S, Lin X, Wu J, Li L, Zhao J and Zhao Y. Neuroprotection of tanshinone IIA against cerebral ischemia/reperfusion injury through inhibition of macrophage migration inhibitory factor in rats. PLoS One 2012; 7: e40165.
[24] Tsai YT, Loh SH, Lee CY, Lee SP, Chen YL, Cheng TH and Tsai CS. Tanshinone IIA inhibits high glucose-induced collagen synthesis via nuclear factor erythroid 2-related factor 2 in cardiac fibroblasts. Cell Physiol Biochem 2018; 51: 2250-2261.
[25] Naci D and Aoudjit F. Alpha2beta1 integrin promotes T cell survival and migration through the concomitant activation of ERK/Mcl-1 and p38 MAPK pathways. Cell Signal 2014; 26: 2008-2015.
[26] Wynn TA. Cellular and molecular mechanisms of fibrosis. J Pathol 2008; 214: 199-210.
[27] Usher KM, Zhu S, Mavropalias G, Carrino JA, Zhao J and Xu J. Pathological mechanisms and therapeutic outlooks for arthrofibrosis. Bone Res 2019; 7: 9.
[28] Zhao H, Wang Y, Qiu T, Liu W and Yao P. Autophagy, an important therapeutic target for pulmonary fibrosis diseases. Clin Chim Acta 2020; 502: 139-147.
[29] Yang Z and Klionsky DJ. Eaten alive: a history of macroautophagy. Nat Cell Biol 2010; 12: 814-822.
[30] Cosin-Roger J, Canet F, Macias-Ceja DC, Gisbert-Ferrándiz L, Ortiz-Masiá D, Esplugues JV, Alós R, Navarro F, Barrachina MD and Calatayud S. Autophagy stimulation as a potential strategy against intestinal fibrosis. Cells 2019; 8: 1078.
[31] Liu H, Fang S, Wang W, Cheng Y, Zhang Y, Liao H, Yao H and Chao J. Macrophage-derived MCPIP1 mediates silica-induced pulmonary fibrosis via autophagy. Part Fibre Toxicol 2016; 13: 55.
[32] Du S, Li C, Lu Y, Lei X, Zhang Y, Li S, Liu F, Chen Y, Weng D and Chen J. Dioscin alleviates crystalline silica-induced pulmonary inflammation and fibrosis through promoting alveolar macrophage autophagy. Theranostics 2019; 9: 1878-1892.
[33] Lu J, Shan J, Liu N, Ding Y and Wang P. Tanshinone IIA can inhibit angiotensin II-induced proliferation and autophagy of vascular smooth muscle cells via regulating the MAPK signaling pathway. Biol Pharm Bull 2019; 42: 1783-1788.
[34] Alenzi FQ. Links between apoptosis, proliferation and the cell cycle. Br J Biomed Sci 2004; 61: 99-102.
[35] Tseng PY, Lu WC, Hsieh MJ, Chien SY and Chen MK. Tanshinone IIA induces apoptosis in human oral cancer KB cells through a mitochondria-dependent pathway. Biomed Res Int 2014; 2014: 540516.
[36] Watanabe T, Noritake J and Kaibuchi K. Regulation of microtubules in cell migration. Trends Cell Biol 2005; 15: 76-83.
[37] Zhang Y, Zhang S and Chen X. Tanshinone IIA protects against cardiac fibrosis through inhibition of beta-tubulin expression. J Biol Regul Homeost Agents 2018; 32: 1451-1455.
[38] Wang Z, Li J, Zhang J and Xie X. Sodium tanshinone IIA sulfonate inhibits proliferation, migration, invasion and inflammation in rheuma-

toid arthritis fibroblast-like synoviocytes. Int Immunopharmacol 2019; 73: 370-378.
[39] Rabanal-Ruiz Y, Otten EG and Korolchuk VI. mTORC1 as the main gateway to autophagy. Essays Biochem 2017; 61: 565-584.
[40] Saxton RA and Sabatini DM. mTOR signaling in growth, metabolism, and disease. Cell 2017; 169: 361-371.
[41] Gui YS, Wang L, Tian X, Li X, Ma A, Zhou W, Zeng N, Zhang J, Cai B, Zhang H, Chen JY and Xu KF. mTOR overactivation and compromised autophagy in the pathogenesis of pulmonary fibrosis. PLoS One 2015; 10: e0138625.
[42] Jiang Y, Hu F, Li Q, Shen C, Yang J and Li M. Tanshinone IIA ameliorates the bleomycin-induced endothelial-to-mesenchymal transition via the Akt/mTOR/p70S6K pathway in a murine model of systemic sclerosis. Int Immunopharmacol 2019; 77: 105968.